JOURNAL OF MATERIALS SCIENCE 8 (1973) 993–999

The constituents of $BaO{\cdot}5.5\ Fe_2O_3$ magnets

LYNN J. BRADY
CTS Corporation, Elkhart, Indiana, USA

Because $BaO{\cdot}5.5\ Fe_2O_3$ magnets have higher $(B_dH_d)_m$ values than comparable $BaFe_{12}O_{19}$ products, magnetic phase analyses were made to find the reason for this characteristic difference. These analyses led to the discovery of a new complex ferrite, $BaFe_{IV}B = Ba_3Fe_4^{2+}Fe_{28}^{3+}O_{49}$. Specimens of this material were found to have the following characteristics at room temperature: $4\pi M_S = 5000$ G and $H^A = 19.3$ kOe. The Curie temperature is 451 °C. These analyses indicated that $BaO{\cdot}5.5\ Fe_2O_3$ specimens are comprised of $\frac{1}{3}$ part $BaFe_{12}O_{19}$ and $\frac{2}{3}$ part $BaFe_{IV}B$ by weight. This explains why $BaO{\cdot}5.5\ Fe_2O_3$ magnets have higher $(B_dH_d)_m$ values than comparable $BaFe_{12}O_{19}$ products.

1. Introduction

Ferrite magnets made commercially with the composition, $BaO{\cdot}5.5\ Fe_2O_3$, usually have higher maximum energy products $(B_dH_d)_m$, than comparable $BaFe_{12}O_{19}$ specimens. Although this can be explained only on the basis of differences in the magnetic characteristics of the materials comprising these magnets, the constituents of $BaO{\cdot}5.5\ Fe_2O_3$ products have never been established. This may be attributed to the extreme complexity [1] of the $BaO\text{-}Fe_2O_3\text{-}FeO$ system and to the lack of adequate analytical methods.

X-ray analysis can usually be employed to determine the materials comprising a magnet, but when all of the magnetic particles in the specimen have the magnetoplumbite structure, as is the case with the barium ferrites; it is difficult to identify these particles on a quantitative basis. A special procedure [2] using X-ray diffraction to differentiate the magnetic barium ferrites was used to derive the phase diagram for the $BaO\text{-}Fe_2O_3\text{-}FeO$ system [3] and still most of the eleven magnetic barium ferrites listed [1] were overlooked. Moreover, this diagram indicates that when specimens of $BaFe_{II}W = BaFe_2^{2+}Fe_{16}^{3+}O_{27}$ are fired in air the resultant product consists of $BaFe_{12}O_{19}$ and Fe_2O_3. This, of course, is a variance with the findings of others [4].

When only standard methods of X-ray analyses were used to establish the phase diagram [5], none of the complex ferrites were identified. However, this diagram shows that certain amounts of BaO dissolves in $BaFe_{12}O_{19}$. Obviously, this could also be interpreted as indicating that these compositions contain $BaFe_{12}O_{19}$ and a complex ferrite with the hexagonal structure whose BaO content is greater than that found in $BaFe_{12}O_{19}$.

Under the circumstances it is not surprising to find that methods to analyse mixtures of $BaFe_{12}O_{19}$ and $BaFe_{II}U = Ba_4Fe_2^{2+}Fe_{36}^{3+}O_{60}$ are unknown. Nevertheless, this is a deplorable situation; because $BaFe_{II}U$ is "nearest neighbour" of $BaFe_{12}O_{19}$ on its BaO rich side of the $BaO\text{-}Fe_2O_3\text{-}FeO$ phase diagram. As a consequence $BaFe_{II}U$ or its oxidation product would be expected to be found in $BaO{\cdot}5.5\ Fe_2O_3$ specimens to preserve stoichiometry, since it is common knowledge that these magnets contain only materials with the magnetoplumbite structure.

A careful consideration of these facts led to the use of magnetic phase analysis to determine the constituents of commercial type $BaO{\cdot}5.5\ Fe_2O_3$ magnets. The results of these analyses are given in this report to explain why these magnets have higher $(B_dH_d)_m$ values than comparable $BaFe_{12}O_{19}$ products.

2. Outline of the experimental procedure

Since the saturation magnetic moment per cm^3, M_S, or the saturation magnetization as it is usually called, is a structure insensitive property of materials [6]; it is well suited to magnetic phase analysis. Thus, it is found that when phase changes occur in magnetic alloys or when compounds are formed sharp breaks are observed in the plots of M_S versus composition [7].

On the other hand, when solid solutions are formed the saturation magnetization changes smoothly with composition [8].

A careful consideration of these phenomena led to the use of magnetic phase diagrams to identify the constituents of $BaO{\cdot}5.5\ Fe_2O_3$ magnets. It was recognized, however, that the saturation magnetization of some alloy specimens is changed by the heat treatment it receives [9] and; consequently, a supplementary analytical method was needed. It was apparent also that the standard powder method of X-ray analysis had little quantitative value in a system as complex as that of $BaO\text{-}Fe_2O_3\text{-}FeO$ and, consequently, could not satisfy this need.

It was found, however, that by using the standard powder method in conjunction with the procedure given [2] to identify some of the hexagonal ferrites, a satisfactory method was derived to supplement magnetic phase analysis. This method is based on the procedure used [10] to identify substances by the powder method, but dual X-ray diffraction patterns of a specimen are employed instead of the single pattern normally used. One of the patterns required by the method is obtained from a powdered non-oriented sample of the specimen. The second pattern, however, is derived from a powdered sample in oriented form.

The analytical procedures indicated, magnetic phase and dual X-ray diffraction, were applied to specimens whose compositions were as follows: $BaO{\cdot}5.5\ Fe_2O_3$; BaM = $BaFe_{12}O_{19}$; $BaFe_{II}U$ = $4BaO{\cdot}19\ Fe_2O_3$; $BaFe_{II}W$ = $BaO{\cdot}9\ Fe_2O_3$; and $\delta BaM{\cdot}(1\text{-}\delta)BaFe_{II}U$. In these symbolic formulas for the complex ferrites, the Roman numeral subscript indicates the number of ferrous ions normally ascribed to the compound [11].

Specimens with these compositions were chosen for the investigation to satisfy both the stoichiometric requirements of $BaO{\cdot}5.5\ Fe_2O_3$ magnets and the conclusions drawn from X-ray analyses. The $BaFe_{II}U$ and $BaFe_{II}W$ specimens, understandably, received preference over other complex ferrites that could have been selected because of their positions in the $BaO\text{-}Fe_2O_3\text{-}FeO$ phase diagram. Thus, it was theorized that, if necessary, $BaFe_{II}X$ = $2BaO{\cdot}15\ Fe_2O_3$, could be synthesized from calcines of BaM and $BaFe_{II}W$ mixed together in the proper proportions. Similarly, it was reasoned that $BaO{\cdot}5.5\ Fe_2O_3$ magnets could be made from calcines of BaM and $BaFe_{II}U$. The $\delta BaM{\cdot}(1\text{-}\delta)BaFe_{II}U$ specimens were prepared to prove this point.

3. Preparation of the specimens

The specimens for the investigation were made using procedures and materials commonly employed by the ferrite industry to ensure production of commercial type $BaO{\cdot}5.5\ Fe_2O_3$ magnets. Technical grade $BaCO_3$ was first dry-mixed with M-25 iron oxide [12] in the proportions required to produce calcines of $BaO{\cdot}5.5\ Fe_2O_3$, BaM, $BaFe_{II}U$ and $BaFe_{II}W$, respectively. After thorough mixing, water and binders were added to a given mix and the resultant product extruded. The extruded material was dried, then calcined in air at 1385°C with a 2 h soak period at peak temperature. The heating and cooling rates of the periodic kiln used were set at 100°C h^{-1}.

Samples of the calcines produced were taken for chemical and X-ray analyses and for microscopic examinations. Inspections showed that each calcine consisted of a single detectable phase and that only materials with the magnetoplumbite structure were present. The impurities found by chemical analyses, after allowances are made for the addition of fluxes, are reported as a footnote of Table I.

The specimens of $\delta BaM{\cdot}(1\text{-}\delta)\ BaFe_{II}U$ were produced from mixtures of BaM and $BaFe_{II}U$ calcines blended together in the desired proportions. In all cases the magnets were made by charging calcined products and small quantities of PbO and SiO_2 into individual jar mills and wet ball-milling the resultant charges until the average size of the ferrite particles approached 1 μm. The PbO and SiO_2 were used as fluxes following accepted industrial practice. After the milling operation, binders and lubricants were added to the jar mills. The resultant charges were then thoroughly mixed by additional milling before discharging the mills and drying the products.

Moulding powders were made from the dried products and these were pressed into the form of rectangular bars using pressures of 460 kg cm^{-2}. These bars were sintered in air at 1200 to 1285°C with soak periods at peak temperature of 2 and 48 h, respectively. The heating and the cooling rates of the periodic kiln were set at 100°C h^{-1}.

The calcining procedure and the sintering schedule employed with the specimens held at peak temperature for 2 h correspond to the industrial practice followed to obtain $BaO{\cdot}5.5\ Fe_2O_3$ and $BaFe_{12}O_{19}$ magnets with the highest attainable $(B_dH_d)_m$ values. They were, therefore,

adopted for the investigation after verifying their values.

Chemical analyses showed that neither the calcines nor the magnets produced contained more than trace amounts of ferrous iron. These results confirmed previous analyses [5]. X-ray diffraction data indicated, however, that only materials with the magnetoplumbite structure were present in these products. It was concluded, therefore, that the complex ferrite calcines and specimens produced were metal deficient compounds. This conclusion coincides with the opinion formed by others [4] who showed that crystallographically pure $BaFe_{II}W$ can be produced with varying ferrous iron contents and no other divalent metal present. It was claimed [4] that the ferrous iron content of this metal deficient compound had little effect on its saturation magnetization. Thus, it was reported that, $M_s = 318$ G, for this material. This compares well with, $M_s = 314$ G, given [13] for single-crystal $BaFe_{II}W$ at room temperature.

4. Magnetic measurements

The magnetic characteristics of the specimens prepared were determined by means of a Magnemetrics Hysteresisgraph with pole coils. Full intrinsic hysteresis loops, as well as second quadrant demagnetization curves were obtained with an accuracy within $\pm$ 1.0%. Portions of typical hysteresis loops displayed by $BaFe_{II}W$ specimens are portrayed in Fig. 1. This figure illustrates the method used [14] to establish the values of $4\pi M_e$, $4\pi M_h$ and $H_i^A/2$ for the magnets. These M_e and M_h terms will be used later to calculate the $4\pi M_s$ value for the specimen.

The hysteresis loop for the easy direction of magnetization of the rectangular specimen is first obtained in fields of $\pm$ 10 kOe, maximum. The specimen is then removed from the equipment without changing the distance between pole pieces appreciably. Next the base line is established. By repeating this procedure for the hard direction, the hysteresis loop and the base line for the hard direction are obtained.

Fig. 1 shows that the intrinsic hysteresis loop for the easy direction of magnetization becomes parallel to its base line at the point indicated by the arrow. Since the field at this point, $H = H_i^A/2$, corresponds very closely to the published value [13] of $H^A/2$, where H^A is the anisotropy field; H_i^A is referred to as the "indicated" anisotropy field. The hysteresis loop for the hard

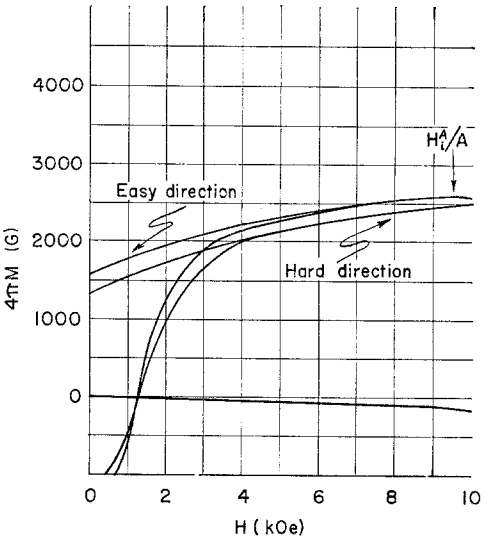

Figure 1 Portions of typical intrinsic hysteresis loops of $BaFe_{II}W$ specimens.

direction does not exhibit this behaviour. This is illustrated dramatically by Fig. 2 which reproduces portions of the intrinsic hysteresis loops of an oriented $BaFe_{12}O_{19}$ magnet.

$4\pi M_e$ equals the difference in values of $4\pi M$ at the intrinsic hysteresis loop for the easy direction of magnetization and its base line when $H = H_i^A/2$. This is illustrated by Fig. 2. The value of $4\pi M_h$ at $H = H_i^A/2$ is obtained in the same

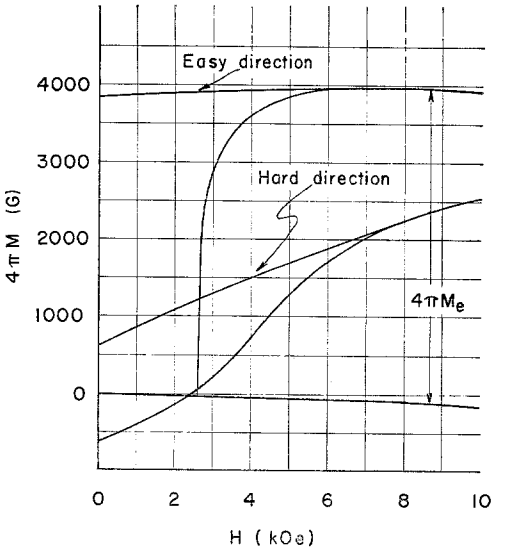

Figure 2 Portions of the intrinsic hysteresis loops of an oriented $BaFe_{12}O_{19}$ magnet.

TABLE I The properties of the specimens*

Type specimen		BaM† (wt %)	Density (g cm^{-3})	$4\pi M_e$ (G)	$4\pi M_h$ (G)	$(B_dH_d)_m$ (MG-Oe)	B_r (G)	H_{ic} (Oe)
BaM	(a)	100	5.00	3215	3085	0.93	2240	1610
BaM	(b)	100	5.02	3220	3160	0.63	2040	1320
$BaFe_{II}W$	(a)	–0–	4.89	2570	2540	0.60	1650	2370
$BaFe_{II}W$	(b)	–0–	5.00	2655	2560	0.58	1690	1910
$BaFe_{II}W$	(c)	–0–	5.07	2630	2620	0.58	1500	1900
$BaO{\cdot}5.5Fe_2O_3$	(a)	—	4.97	3290	3160	1.07	2280	2180
$BaO{\cdot}5.5Fe_2O_3$	(a)	—	4.99	3310	3190	1.06	2270	2180
BaM-$BaFe_{II}U$	(a)	–0–	5.03	3160	2920	0.87	2060	2300
BaM-$BaFe_{II}U$	(a)	25	5.02	3210	3100	1.02	2200	2380
BaM-$BaFe_{II}U$	(a)	50	4.95	3310	3200	1.06	2240	2240
BaM-$BaFe_{II}U$	(a)	67	4.96	3310	3140	1.08	2220	2250
BaM-$BaFe_{II}U$	(a)	75	5.03	3290	3180	1.08	2270	2200
BaM-$BaFe_{II}U$	(a)	100	4.91	3200	3010	0.96	2200	1950

(a) 2 h at 1250°C, (b) 48 h at 1250°C, (c) 48 h at 1285°C.
*Contain 2.8% non-magnetic impurities; †impurity content not considered.

TABLE II Comparing the calculated and published values of $4\pi M_s$ and H^A of the specimens

Type specimen		BaM (wt %)	Theoretical density (g cm^{-3})	$H_i{}^A$ (kOe)	H^A published (kOe)	$4\pi M_s$ calculated (G)	$4\pi M_s$ published (G)
BaM	(b)	100	5.28 (5)	17.3	17.1 (17)	4775	4775 (17)
BaM	(c)	100	5.28 (5)	17.3	17.1 (17)	4815	4775 (17)
$BaFe_{II}W$	(a)	–0–	5.31 (5)	19.0	19.0 (13)	3985	3995 (4) (*)
$BaFe_{II}W$	(b)	–0–	5.31 (5)	19.0	19.0 (13)	3965	3945 (13) (†)
$BaFe_{II}W$	(c)	–0–	5.31 (5)	19.0	19.0 (13)	3955	3945 (13) (†)
$BaO{\cdot}5.5Fe_2O_3$	(a)	—	5.29	19.3	—	4925	—
$BaO{\cdot}5.5Fe_2O_3$	(a)	—	5.29	19.3	—	4940	—
BaM-$BaFe_{II}U$	(a)	–0–	5.31 (5)	20.0	—	4590	—
BaM-$BaFe_{II}U$	(a)	25	5.30	19.3	—	4780	—
BaM-$BaFe_{II}U$	(a)	50	5.30	19.3	—	5000	—
BaM-$BaFe_{II}U$	(a)	67	5.29	19.3	—	4930	—
BaM-$BaFe_{II}U$	(a)	75	5.29	18.7	—	4895	—
BaM-$BaFe_{II}U$	(a)	100	5.28 (5)	17.3	17.1 (17)	4785	4775 (17)

(a), (b) and (c), see Table I
(*) Polycrystalline sample; (†) single-crystal value.

manner from the hysteresis loop and the base line for the hard direction.

Table I gives the observed magnetic characteristics of the specimens including the values of $4\pi M_e$ and $4\pi M_h$ obtained as outlined. The reported values of $(B_dH_d)_m$, the residual induction, B_r, and the intrinsic coercive force, H_{ci}, are those obtained parallel to the pressing direction and, hence, correspond to those usually given for ferrite magnets. This table also lists the density values of the specimens. These were obtained by displacement methods and are regarded as accurate to $\pm$ 0.1%.

5. Deriving the $4\pi M_s$ values

The $4\pi M_s$ values of the specimens were calculated using the following equation and pertinent data from Tables I and II [14]:

$$(M_e + M_h)/2 = M_s f\left[\frac{9}{4\pi} + \left(\frac{3}{4} - \frac{9}{4\pi}\right)\left(\frac{M_e}{M_h} - 1\right)\right]. \quad (1)$$

This equation is based on finding that the theoretical demagnetization curve of an isotropic rectangular shaped $BaFe_{12}O_{19}$ specimen passes through the point ($H = H^A/2$, $M = 9M_s/4\pi$), as the field strength is reduced from $H/H^A = 0{\cdot}8$ to 0. It is also based on the relationship, $(M_e + M_h)/2 = 3M_s/4$ for a theoretical, completely oriented, rectangular specimen placed in a field $H = H^A/2$. By using these results, Equation 1 was derived on the assumption that a linear relationship

exists between the orientation of the specimen and its average magnetization value $(M_e + M_h)/2$, at $H = H^A/2$.

The purity factor, f, in Equation 1 is equal to the product of the chemical purity of the specimen, expressed as a decimal fraction, and its relative density. The published "theoretical" or X-ray densities of BaM, $BaFe_{II}U$ and $BaFe_{II}W$ magnets are, therefore, provided in Table II for these calculations. This table also gives the "theoretical" densities of the BaO·5.5 Fe_2O_3 and $\delta BaM\cdot(1-\delta)BaFe_{II}U$ specimens. These values were calculated on the assumption that linear relationships exist between the compositions and the densities of these specimens.

In deriving the M_s values by means of Equation 1, it was assumed that the chemical purity of the specimen is equal to the sum of the impurities found in the calcines and the combined amounts of PbO and SiO_2 added as fluxes. This assumption is reasonable, since the magnetic properties of lead and barium ferrites are roughly equivalent [15] and consequently mutual metathesis of the lead silicates and barium ferrites can have little effect on the M_s of the specimen when the amount of PbO used is small. The use of PbO does introduce a possible error however, since lead compounds are volatile at high temperatures.

Table II gives the calculated values of $4\pi M_s$ for the specimens as well as those published for BaM and $BaFe_{II}W$. It is seen that agreement between the calculated and published values is excellent. This table also shows that agreement between H_i^A and H^A for these compounds is very good.

The data in Table II indicate that unlike some magnetic alloys [9] the M_s values of BaM and $BaFe_{II}W$ specimens are not effected by the sintering time or temperature used to make these products. Unreported results show the same effects for $\delta BaM\cdot(1-\delta)$ $BaFe_{II}U$ magnets. This, obviously, makes it easier to interpret the phase diagram.

6. The magnetic phase diagram

The magnetic phase diagram of the $\delta BaM\cdot(1-\delta)$ $BaFe_{II}U$ system is portrayed in Fig. 3. This diagram was constructed by plotting the $4\pi M_s$ values of the $\delta BaM\cdot(1-\delta)BaFe_{II}U$ magnets reproduced in Table II against composition. Included in this figure, for purposes of comparison, are the $4\pi M_s$ values of the BaO·5.5 Fe_2O_3 specimens. These values, 4925 and 4940 G, respectively, are found within the circle cut by the left-hand branch of the phase diagram. Included in this circle at $4\pi M_s = 4930$ G, is the $4\pi M_s$ value of the magnet made from $\frac{2}{3}$ part BaM and $\frac{1}{3}$ part $BaFe_{II}U$ calcines by weight.

The sharp break in the magnetic phase diagram at $4\pi M_s = 5000$ G suggests that an unreported compound is formed in the BaO-Fe_2O_3-FeO system. For reference purposes this hypothetical compound is designated $BaFe_{IV}B$. In order to verify its existence, specimens of BaM, $BaFe_{II}U$ and $BaFe_{IV}B$ were prepared for dual X-ray analyses. These specimens were made from reagent grade $BaCO_3$ and Fe_2O_3 thoroughly mixed together in the proportions required to produce the respective compounds. No PbO, SiO_2, binders or lubricants were used in these preparations. The "green" specimens prepared were sintered adjacent to each other in air to 1385°C with a 5 h soak period at peak temperature. The heating and cooling rates of the kiln were set at 100°C h^{-1}.

Powdered samples of the specimens were prepared in both oriented and non-oriented forms. Diffraction patterns of these were obtained by means of Siemens' Crystalloplex IV X-ray diffraction equipment employing a 5.73 cm Debye-Scherrer camera and Cu$K\alpha$ radiation. The data derived from the patterns are shown in Table III.

The formation of the compound, $BaFe_{IV}B$, was confirmed by means of these data and the procedure used [10] to identify substances by the powder method. Its empirical chemical formula was then established on the assumptions that the composition of $BaFe_{IV}B$ is 3BaO·16 Fe_2O_3 and

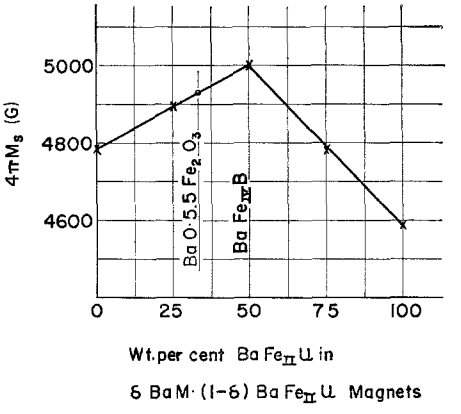

Figure 3 The magnetic phase diagram of the $\delta BaM\cdot(1-\delta)BaFe_{II}U$ system.

TABLE III Dual X-ray diffraction data for specimens of BaM, $BaFe_{IV}B$ and $BaFe_{II}U$

d-spacing (Å)	$100\ I/I_{max}$					
	Non-oriented specimens			Oriented specimens		
	BaM	$BaFe_{IV}B$	$BaFe_{II}U$	BaM	$BaFe_{IV}B$	$BaFe_{II}U$
3.10	—	—	110	—	—	60
2.89	10	50	10	2	100	15
2.77	40	50	—	60	—	—
2.71	—	—	50	—	—	70
2.61	—	80	—	—	60	—
2.59	60	—	50	30	—	60
2.40	30	30	15	10	20	20
2.11	20	10	30	—	10	15
2.04	—	5	30	—	—	15
1.80	15	8	2	2	—	—
1.66	40	80	100	30	50	100
1.622	—	100	100	—	60	100
1.612	100	—	—	100	—	—
1.465	90	95	70	80	80	80
1.379	20	10	7	—	—	—
1.293	50	30	10	30	10	20
1.249	2	—	20	—	—	20

that its crystallographic structure, in symbolic notation [16], corresponds to MYS. The composition was derived from the phase diagram shown in Fig. 3, while the MYS structure was chosen because it meets stoichiometric requirements.

On the basis of these assumptions, the empirical chemical formula, $Ba_3Fe_4^{2+}Fe_{28}^{3+}O_{49}$, was assigned to the newly discovered complex ferrite, $BaFe_{IV}B = 3BaO{\cdot}16Fe_2O_3$. Specimens with this composition are, accordingly, reported to have the following characteristics at room temperature: $4\pi M_S = 5000$ G and $H_i^A = 19.3$ kOe. The Curie temperature is 451 °C.

7. Conclusions

The magnetic phase diagram of the δBaM·(1-δ) $BaFe_{II}U$ system shows no sign of solid solution formation. However, it does indicate the composition of the newly discovered complex ferrite, $BaFe_{IV}B = Ba_3Fe_4^{2+}Fe_{28}^{3+}O_{49}$ and gives its $4\pi M_S$ value as 5000 G at room temperature. It shows, too, that linear relationships exist between the $4\pi M_S$ values and the composition of specimens of BaM and $BaFe_{IV}B$ or of $BaFe_{IV}B$ and $BaFe_{II}U$. On the basis of these relationships and the experimental results that have been reported, it is postulated that BaO·5.5 Fe_2O_3 magnets are comprised of $\frac{1}{3}$ part BaM and $\frac{2}{3}$ part $BaFe_{IV}B$ by weight. This explains why commercial BaO·5.5 Fe_2O_3 magnets processed under ideal conditions have higher $(B_dH_d)_m$ values than comparable $BaFe_{12}O_{19}$ products.

Acknowledgements

I wish to acknowledge the help of Professor Albert E. Miller of Notre Dame University who made the Curie point measurements. I am grateful to Jack Rentschler of the Homer Laboratories, Bethlehem Steel Corporation, for the numerous X-ray diffraction data he obtained. I also wish to thank the St Joe Minerals Corporation for the use of their equipment in this investigation. In addition, I wish to express my appreciation to Delores M. Estes and Curtis L. Holmes of CTS Corporation who obtained the X-ray diffraction patterns.

References

1. G. WINKLER, "Reactivity of Solids", ed. G. M. Schwab (Elsevier, New York, 1965) p. 572.
2. J. SMIT and H. P. J. WIJN, "Ferrites" (Wiley, New York, 1959) p. 189.
3. H. J. VAN HOOK, *J. Amer. Ceram. Soc.* **47** (1964) 579. "Phase Diagrams for Ceramists, 1969 Supplement," compiled by Ernest M. Levin, Carl R. Robbins and Howard F. McMardie; Margie K. Reser, Editor (The American Ceramic Society, Columbus, Ohio, 1969) p. 16.
4. H. NEUMANN and H. P. J. WIJN, *J. Amer. Ceram. Soc.* **51** (1968) 536.

5. YASUMASA GOTO and TOSHIO TAKADA, *ibid* **43** (1960) 150.
6. RICHARD M. BOZORTH, "Ferromagnetism" (Van Nostrand, New York, 1953) p. 15.
7. *Ibid*, p. 37 and Figs. 7-8, 8-75 and 8-79.
8. *Ibid*, Figs. 6-5 and 8-76.
9. *Ibid*, Figs. 8-62.
10. LEONID V. AZAROFF and MARTIN J. BUERGER, "The Powder Method in X-ray Crystallography" (McGraw-Hill, New York, 1958) p. 181.
11. A. D. WADSLEY, "Non-Stoichiometric Compounds", ed. L. Mandelcorn (Academic Press, New York, 1964) p. 149.
12. St Joe Minerals Corporation, 250 Park Avenue, New York.
13. J. J. WENT, G. W. RATHENAU, E. W. GORTER, and G. W. VAN OOSTERHOUT, *Philips Tech. Rev.* **13** (1951/1952) 194 as cited by J. SMIT and H. P. J. WIJN, "Ferrites", p. 204.
14. LYNN J. BRADY, unpublished.
15. MICHAEL TOKAR, *J. Amer. Ceram. Soc.* **52** (1969) 302.
16. J. SMIT and H. P. J. WIJN, "Ferrites," p. 177.
17. B. T. SHIRK and W. R. BUESSEM, *J. Appl. Phys.* **40** (1969) 1294.

Received 14 November 1972 and accepted 19 February 1973.